J Biol Inorg Chem (2007) 12:667–679
DOI 10.1007/s00775-007-0215-0

ORIGINAL PAPER

A new bisphosphonate-containing ^{99m}Tc(I) tricarbonyl complex potentially useful as bone-seeking agent: synthesis and biological evaluation

Elisa Palma · Bruno L. Oliveira · João D. G. Correia · Lurdes Gano · Leonor Maria · Isabel C. Santos · Isabel Santos

Received: 14 November 2006 / Accepted: 28 January 2007 / Published online: 2 March 2007
© SBIC 2007

Abstract Aiming to develop new bone-seeking radiotracers based on the organometallic core *fac*-[^{99m}Tc(CO)$_3$]$^+$ with improved radiochemical and biological properties, we have prepared new conjugates with phosphonate pendant groups. The conjugates comprise a chelating unit for metal coordination, which corresponds to a pyrazolyl-containing backbone (pz) with a N,N,N donor-atom set, and a pendant diethyl phosphonate (pz-MPOEt), phosphonic acid (pz-MPOH) or a bisphosphonic acid (pz-BPOH) group for bone targeting. Reactions of the conjugates with the precursor [^{99m}Tc(H$_2$O)$_3$(CO)$_3$]$^+$ yielded (mote than 95%) the single and well-defined radioactive species [^{99m}Tc(CO)$_3$(κ^3-pz-MPOEt)]$^+$ (**1a**), [^{99m}Tc(CO)$_3$(κ^3-pz-MPOH]$^+$ (**2a**) and [^{99m}Tc(CO)$_3$(κ^3-pz-BPOH)]$^+$ (**3a**), which were characterized by reversed-phase high-performance liquid chromatography . The corresponding Re surrogates (**1**–**3**), characterized by the usual analytical techniques, including X-ray diffraction analysis in the case of **1**, allowed for macroscopic identification of the radioactive conjugates. These radioactive complexes revealed high stability both in vitro (phosphate-buffered saline solution and human plasma) and in vivo, without any measurable decomposition. Biodistribution studies of the complexes in mice indicated a fast rate of blood clearance and high rate of total radioactivity excretion, occurring primarily through the renal–urinary pathway in the case of complex **3a**. Despite presenting moderate bone uptake (3.04 ± 0.47% injected dose per gram of organ, 4 h after injection), the high stability presented by **3a** and its adequate in vivo pharmacokinetics encourages the search for new ligands with the same chelating unit and different bisphosphonic acid pendant arms.

Keywords Technetium-99m · Rhenium · Bisphosphonate · Bone · Radiopharmaceuticals

Abbreviations

Boc	*tert*-Butoxycarbonyl
BP	Bisphosphonate
COSY	Correlation spectroscopy
DCC	*N*,*N*′-Dicyclohexylcarbodiimide
HMDP	Hydroxymethylenediphosphonate
HOBt	1-Hydroxybenzotriazole
HPLC	High-performance liquid chromatography
HSQC	Heteronuclear single quantum coherence
ID	Injected dose
MDP	Methylenediphosphonate
MP	Monophosphonate
pz	Pyrazolyl-containing backbone
RP	Reversed phase

Introduction

One of the most important clinical procedures for assessing bone damage (e.g., arthritis, osteoporosis or skeletal metastases), infection or injury (e.g., fractures) in the whole body is radionuclide bone imaging with specific radiotracers [1]. Besides skeletal imaging, certain bone-seeking radiotracers are widely used for radionuclide therapy of bone malignancies. In fact, breast and prostate carcinomas often produce metastatic bone lesions which, in

E. Palma · B. L. Oliveira · J. D. G. Correia · L. Gano · L. Maria · I. C. Santos · I. Santos (✉)
Departamento de Química,
ITN, Estrada Nacional 10,
2686-953 Sacavém Codex, Portugal
e-mail: isantos@itn.pt

most cases, lead to intractable and debilitating pain [2, 3]. In the case of widespread bone metastases, systemic radionuclide therapy with β-emitting radiopharmaceuticals (e.g., ^{89}Sr, ^{186}Re and ^{153}Sm) is a well-established procedure for the management of painful bone metastases and palliative treatment, and is a subject of intense research [4–11].

Simple bisphosphonate (BP) compounds, which contain the P–C–P backbone, have been developed as stable analogues of inorganic polyphosphates/pyrophosphates, and have been used in the preparation of ^{99m}Tc radiopharmaceuticals for bone imaging since the mid-1970s [1, 12].

Nowadays, the most used BP-containing radiopharmaceuticals for bone imaging are ^{99m}Tc-MDP (MDP is methylenediphosphonate) and ^{99m}Tc-HMDP (HMDP is hydroxymethylenediphosphonate) analogues (Structure 1).

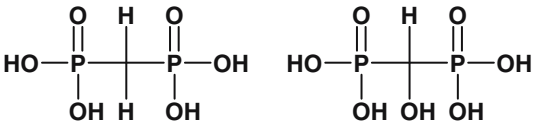

These ^{99m}Tc-BP radiopharmaceuticals do not present single, well-defined chemical species, but mixtures of short-chain and long-chain polymers, which may reduce the efficacy of the radiopharmaceutical. The biological behavior of this type of tracer is also affected by the different degrees of ionization presented by the different polymers, and by the variation of the relative amounts of the polymers over time, after preparation. Another disadvantage associated with the ^{99m}Tc-BPs is related to their in vivo instability, which may lead to the oxidation of the metal to pertechnetate ($[^{99m}TcO_4]^-$). Moreover, the ^{99m}Tc-BPs present a relatively slow blood and soft-tissue clearance, delaying the start of the bone-scanning procedure in nuclear medicine centers [13].

The drawbacks associated with the ^{99m}Tc-BPs in clinical use show that there is space for the development of new bone-seeking radiotracers based on ^{99m}Tc with better chemical and biological properties. The attempts made in the past few years to achieve that goal comprise both the direct labeling of new BPs with ^{99m}Tc, leading, still, to noncharacterized mixtures of polymers [14–16], and the use of a ^{99m}Tc(V) mono-oxo complex stabilized by a bifunctional tetradentate ligand with a pendent aminomethylenediphosphonate unit, which has promising biological properties [13].

Despite the fact that the organometallic core *fac*-$[^{99m}Tc(CO)_3]^+$ has been successfully used for the labeling of biologically relevant molecules with a large variety of ligands and/or donor-atom sets, this unit has not yet been explored for the labeling of BPs [17–22]. The formation of well-defined single species, and the remarkable stability in vivo and vitro shown by the ^{99m}Tc tricarbonyl biocomplexes anchored by pyrazolyl-containing ligands [21–24], prompted us to explore the possibility of labeling phosphonates with that system, and to assess the biological properties of the resulting radioactive complexes. Herein we describe the synthesis and characterization of a new family of bifunctional ligands with a pyrazolyl-containing backbone (pz), for stabilization of the metallic center, and a monophosphonate (MP)/BP pendant unit, for bone targeting (pz-MPOEt, pzMPOH and pz-BPOH). The preparation, characterization and biological evaluation of the resulting organometallic complexes *fac*-$[M(CO)_3(\kappa^3$-pz-MPOEt)] [M is Re (**1**), ^{99m}Tc (**1a**)], *fac*-$[M(CO)_3(\kappa^3$-pz-MPOH)] [M is Re (**2**), ^{99m}Tc (**2a**)] and *fac*-$[M(CO)_3(\kappa^3$-pz-BPOH)] [M is Re (**3**), ^{99m}Tc (**3a**)] are also described.

Materials and methods

All chemicals and solvents were of reagent grade and were used without purification unless stated otherwise. Diethyl (2-bromoethyl)phosphonate was obtained in high yield (more than 85%) using the classic Michaelis–Arbuzov reaction by refluxing dry triethyl phosphite in a 30-fold excess of dry dibromoethane overnight, followed by vacuum distillation [25]. 1-Aminomethylenediphosphonic acid tetraethyl ester was prepared in two sequential steps as described elsewhere [26, 27]. The organic compounds 3,5-Me_2pz$(CH_2)_2$NH$(CH_2)_2$NH–Boc (Boc is tert-butoxycarbonyl), 3,5-Me_2pz$(CH_2)_2$N$((CH_2)_3$COOH$)(CH_2)_2$–NH–Boc, 3,5-Me_2pz$(CH_2)_2$N$((CH_2)_3$COOH$)(CH_2)_2$–NH_2 (pz–COOH), and the organometallic precursors $(NEt_4)_2[Re(CO)_3Br_3]$, $[Re(CO)_5Br]$ and $[Re(CO)_3(H_2O)_3]Br$ were prepared according to published methods [21–23, 28, 29]. Na$[^{99m}TcO_4]$ was eluted from a ^{99}Mo/^{99m}Tc generator, using 0.9% saline. The radioactive precursor *fac*-$[^{99m}Tc(OH_2)_3(CO)_3]^+$ was prepared using a IsoLink® kit (Malinckrodt). ^{99m}Tc-MDP (better than 98% yield by instant thin-layer chromatography) was prepared by reconstitution of a conventional MDP labeling kit (Nordion) with Na$[^{99m}TcO_4]$. ^{1}H, ^{11}C and ^{31}P NMR spectra were recorded at room temperature using a Varian Unity 300 MHz spectrometer. ^{1}H and ^{11}C chemical shifts were referenced with the residual solvent resonances relative to tetramethylsilane, and the ^{31}P chemical shifts with external 85% H_3PO_4 solution. NMR spectra were obtained in $CDCl_3$, CD_3OD and D_2O. IR spectra were recorded as KBr pellets with a PerkinElmer 577 spectrometer C, H and N analyses were performed using an EA 110 CE Instruments automatic analyser. High-performance liquid chromatography (HPLC) analyses of the Re and ^{99m}Tc complexes were performed both with a PerkinElmer LC pump 200 coupled to an LC 290 tunable

UV–vis detector and to a Berthold LB-507A radiometric detector. Separations were achieved on a Nucleosil column (10 μm, 250 mm × 4 mm), using a flow rate of 1 mL min^{-1}; UV detection, 254 nm; eluent A aqueous 0.1% (pz-MPOEt, pz-MPOH, **1/1a**, **2/2a**)/0.5% (**I**, **II**, **3/3a**) CF_3COOH solution, eluent B acetonitrile (pz-MPOEt, pz-MPOH, **1/1a**, **2/2a**) or 0.5% CF_3COOH solution in acetonitrile (**I**, **II**, **3/3a**); method, t = 0–3 min, 0% eluent B; 3–3.1 min, 0–25% eluent B; 3.1–9 min, 25% eluent B; 9–9.1 min, 25–34% eluent B; 9.1–20 min, 34–100% eluent B; 20–24 min, 100% eluent B; 24–26 min, 100–0% eluent B; 26–30 min, 0% eluent B.

Synthesis of pz(Boc)-MPOEt

To a solution of 3,5-$Me_2pz(CH_2)_2NH(CH_2)_2$–NH–Boc (1.76 g, 6.23 mmol) and diethyl (2-bromoethyl)phosphonate (5.00 g, 20.40 mmol) in CH_3CN (40 mL) were added K_2CO_3 (1.37 g, 9.91 mmol) and a catalytic amount of KI in solid. After 10 days under reflux, the solution was filtered through a pad of Celite, and H_2O and dichloromethane were added to the filtrate. The organic phase was separated, and the aqueous phase was further extracted with dichloromethane (twice). The organic phases were then collected, dried over anhydrous $MgSO_4$ and filtered, and the solvents were evaporated until a viscous residue was obtained. This residue was chromatographed on an appropriate column of silica gel with 8–50% methanol/ethyl acetate (gradient) to afford a pale yellow viscous oil. Yield: 0.96 g, 35%. ^{1}H NMR (CD_3OD, δ): 5.82 [s, H(4)pz, 1H], 4.12–3.98 (m, CH_2, 6H), 3.03 (t, CH_2, 2H), 2.81 (t, CH_2, 2H), 2.73 (q, CH_2, 2H), 2.54 (t, CH_2, 2H), 2.27 (s, CH_3, 3H), 2.16 (s, CH_3, 3H), 1.92–1.82 (m, CH_2, 2H), 1.42 (s, CH_3, 9H), 1.31 (t, CH_3, 6H). ^{31}P NMR (CD_3OD, δ): 32.8.

Synthesis of pz-MPOEt

The Boc protecting group was removed by dissolving pz(Boc)-MPOEt (0.41 g, 0.92 mmol) in CF_3COOH (3 mL), and by stirring for 1 h at room temperature. After evaporation of the solvent, the residue was dissolved in 30% NaOH, and the solution was extracted with dichloromethane (three times). The organic fractions were collected, dried over anhydrous $MgSO_4$ and filtered, and the filtrate was evaporated to dryness. The compound was obtained as a pale yellow oil. Yield: 0.28 g, 88%. ^{1}H–NMR (CD_3OD, δ): 5.82 [s, H(4)pz, 1H], 4.13–4.00 (m, CH_2, 6H), 2.83–2.73 (m, CH_2, 4H), 2.61–2.58 (m, CH_2, 2H), 2.54–2.50 (m, CH_2, 2H), 2.26 (s, CH_3, 3H), 2.16 (s, CH_3, 3H), 1.99–1.86 (m, CH_2, 2H), 1.32 (t, CH_3, 6H). ^{31}P NMR (CD_3OD, δ): 32.8. IR (KBr, ν/cm^{-1}): 1,553, 1,464, 1,206 (P=O), 1,027, 969, 796. Retention time (reversed-phase HPLC, RP-HPLC): 9.5 min.

Synthesis of pz-MPOH

To a solution of pz-MPOEt (0.21 g, 0.48 mmol) in dry dichloromethane (3 mL) at 0 °C was added trimethylsilyl bromide (0.5 mL, 3.6 mmol). After stirring at room temperature for 72 h, the reaction mixture was evaporated, and methanol and water were added to the residue. After stirring during 1.5 h, the solvents were removed by evaporation. The oil obtained gave a white solid after thorough washing with dichloromethane. Yield: 0.11 g, 50%.^{1}H NMR (D_2O, δ): 6.03 [s, H(4)pz, 1H], 4.35 (s br, CH_2, 2H), 3.37 (s br, CH_2, 2H), 3.24–3.15 (m, CH_2, 6H), 2.19 (s, CH_3, 3H), 2.12 (s, CH_3, 3H), 1.89–1.83 (m, CH_2, 2H). ^{13}C NMR (D_2O, δ): 150.9 [C(3/5)pz], 146.1 [C(3/5)pz], 109.5 [C(4)pz], 55.5 (CH_2), 52.3 (CH_2), 45.9 (CH_2), 37.7 (CH_2), 26.8 (CH_2), 25.1 (CH_2), 14.2 (CH_3), 12.7 (CH_3). ^{31}P NMR (D_2O, δ): 20.3. Anal. Calcd for $C_{11}H_{23}N_4O_3P{\cdot}2HBr$: C, 29.22; H, 5.57; N, 12.39. Found: C, 29.42; H, 5.40; N, 12.28. Retention time (RP-HPLC): 8.0 min.

Synthesis of pz(Boc)-BPOEt

To a solution of 3,5-$Me_2pz(CH_2)_2N((CH_2)_3COOH)$ $(CH_2)_2$ NH-Boc (0.100 g, 0.27 mmol) and 1-hydroxybenzotriazole (HOBt; 0.036 g, 0.27 mmol) in acetonitrile (20 mL) at 0–5 °C was added *N*,*N*′-dicyclohexylcarbodiimidae (DCC; 0.055 g, 0.27 mmol), and the mixture was stirred for 30 min. After addition of 1-aminomethylenediphosphonic acid tetraethyl ester (0.082 g, 0.27 mmol) dissolved in acetonitrile (approximately 1 mL), stirring was continued overnight at room temperature. The DCC–urea precipitate was then removed by filtration through a pad of Celite, and the filtrate was evaporated. The residue obtained was purified using an appropriate column of silica gel with 2.5–15% methanol/CH_2Cl_2 (gradient) affording a yellowish oil. Yield: 0.10 g, 58%. ^{1}H NMR ($CDCl_3$, δ): 8.73 (d br, NH, 1H, $^3J_{HH}$ = 9.0), 5.82 [s, H(4)pz, 1H], 5.18 (td, P–CH–P, 1H, $^2J_{PH}$ = 22.2, $^3J_{HH}$ = 10.2), 4.69 (s br, NH, 1H), 4.24–4.00 (m, CH_2, 10H), 2.86 (q br, CH_2, 2H), 2.64 (t br, CH_2, 2H), 2.45 (t br, CH_2, 2H), 2.38 (m, CH_2, 4H), 2.23 (s, CH_3, 3H), 2.21 (s, CH_3, 3H), 1,71 (m, CH_2, 2H), 1,38 (s, CH_3, 9H), 1,26 (m, CH_2, 12H). ^{31}P NMR ($CDCl_3$, δ): 17.5.

Synthesis of pz-BPOH

To a solution of pz(Boc)-BPOEt (0.068 g, 0,104 mmol) in dry dichloromethane (5 mL) at 0 °C was added dropwise trimethylsilyl bromide (1.5 mL, 11 mmol). The mixture was allowed to warm up to room temperature and was stirred for 72 h. The solvent was evaporated, and methanol

was added to the residue (15 mL). After stirring for 1.5 h, the methanol was removed by evaporation and the crude product was purified by precipitation from MeOH using diethyl ether. The precipitate was collected by centrifugation, washed with diethyl ether and dried in a vacuum, yielding pz-BPOH as a white solid. Yield: 0.046 g, 73%. ^{1}H NMR (D_2O, δ): 6.07 [s, H(4)pz, 1H], 4.38 (t, CH, 1H), 3.68–3.07 (m br, CH_2, 10H), 2.38 (s br, CH_2, 2H), 2.20 (s, CH_3, 3H), 2.15 (s, CH_3, 3H), 1.94 (s br, CH_2, 2H). ^{13}C NMR (D_2O, δ): 175.9 (COOH), 150.1 [C(3/5)pz], 147.6 [C(3/5)pz], 109.8 [C(4)pz], 55.5 (CH_2), 53.5 (CH_2), 49.7 (CH_2), 47.9 (CH), 44.4 (CH_2), 37.6 (CH_2), 34.6 (CH_2), 21.6 (CH_2), 13.1 (CH_3), 12.4 (CH_3). ^{31}P NMR (D_2O, δ): 13.7. Anal. Calcd for $C_{14}H_{29}N_5O_7P_2{\cdot}2HBr$: C, 27.88; H, 5.18; N, 11.61. Found: C, 28.25; H, 5.13; N, 11.25. IR (KBr, ν/cm^{-1}): 1,647 (C=O), 1,527, 1,154 (P=O), 1,064, 915.

Synthesis of **1**

To a stirred suspension of $[Re(CO)_5Br]$ (0.036 g, 0.089 mmol) in MeOH was added pz-MPOEt dissolved in the same solvent (0.029 g, 0.13 mmol), and the resulting mixture was refluxed overnight. The residue obtained after evaporation of the solvent was washed (three times) with *n*-hexane, giving a white solid, which was dried under vacuum. Yield: 0.053 g, 96%. ^{1}H NMR (CD_3OD, δ): 6.21 [s, H(4)pz, 1H], 5.57 (q br, NH, 1H), 4.54 (dd, CH, 1H), 4.25–4.13 (m, CH_2, 6H), 3.95–3.88 (m, CH, 1H), 3.80–3.68 (m, NH, 1H), 3.43 (dd, CH, 1H), 3.23–3.19 (m, CH, 1H), 2.96 (d br, CH, 1H), 2.85–2.70 (m, CH_2, 2H), 2.59–2.49 (m, CH_2, 2H), 2.45 (s, CH_3, 3H), 2.38 (s, CH_3, 3H), 2.31–2.28 (m, CH, 1H), 1.37 (t, CH_3, 6H). ^{13}C NMR (CD_3OD, δ): 195.0 (C≡O), 194.7 (C≡O), 193.6 (C≡O), 155.3 [C(3/5)pz], 145.6 [C(3/5)pz], 109.3 [C(4)pz], 64.0 (CH_2), 63.9 (CH_2), 62.1 (CH_2), 61.3 (CH_2), 53.4 (CH_2), 43.5 (CH_2), 23.0 (CH_2), 21.2 (CH_2), 16.8 (CH_3), 16.7 (CH_3), 16.1 (CH_3), 11.6 (CH_3). ^{31}P NMR: δ 29.4. IR (KBr, ν/cm^{-1}): 2,098, 2,027, 1,901 (C≡O), 1,263, 1,023 (P=O), 798, 739. Anal. Calcd for $C_{18}H_{31}N_4O_6PBrRe$: C, 31.04; H, 4.49; N, 8.04. Found: C, 31.30; H, 4.40; N, 7.89. Retention time (RP-HPLC): 15.8 min.

Synthesis of **2**

To a stirred suspension of $[Re(CO)_5Br]$ (0.018 g, 0.044 mmol) in H_2O was added a solution of pz-MPOH (0.020 g, 0.044 mmol) in the same solvent, and the resulting mixture was refluxed overnight. After evaporation of the solvent, the residue obtained was dried under vacuum and analyzed by RP-HPLC and NMR spectroscopy. The crude product revealed a mixture of free pz-MPOH and complex **2**. Yield (**2**, calculated from the ^{1}H NMR spectrum): 36%. ^{1}H NMR (D_2O, δ): 6.01 [s, H(4)pz, 1H], 5.07 (q br, NH, 1H), 4.30 (dd, H, 1H), 4.12–4.03 (m, CH, 1H), 3.74–3.55 (m, CH, NH, 3H), 3.08 (m, CH, 1H), 2.69 (m, CH, 1H), 2.60–2.52 (m, CH, 1H), 2.42–2.32 (m, CH, 1H), 2.25 (s, CH_3, 3H), 2.14 (s, CH_3, 3H). ^{31}P NMR: δ 25.3 (CD_3OD), 23.4 (D_2O). Retention time (RP-HPLC): 10.8 min.

Synthesis of **3**

Direct method

A solution of $[Re(H_2O)_3(CO)_3]Br$ (0.011 g, 0.029 mmol) and pz-BPOH (0.010 g, 0.023 mmol) in H_2O was refluxed overnight. The water was removed under vacuum, and the residue obtained was dissolved again in a H_2O/acetonitrile mixture (90:10). The precipitate formed was eliminated by centrifugation. The resulting supernatant was purified by semipreparative RP-HPLC on a Macherey–Nagel C18 column (Nucleosil 100–7, 250 mm × 8 mm) at a flow rate of 2 mL min^{-1} with a gradient mobile phase of 100% water with 0.5% CF_3COOH to 100% acetonitrile with 0.5% CF_3COOH for 30 min. Chromotograms were obtained by monitoring the UV absorption at a wavelength of 254 nm. Evaporation of the solvent in a vacuum gave **3** as a pale yellow clear oil. Yield: 8.8 mg, 54%.

Indirect method

1. *Synthesis of the precursor* $[Re(CO)_3(\kappa^3\text{-pz-COOH})]^+$ ***(I)*** [23]. $(NEt_4)_2[ReBr_3(CO)_3]$ (0.100 g, 0.131 mmol) was reacted with an equimolar amount of pz–COOH) (0.050 mg, 0.131 mmol) in refluxing H_2O for 18 h. After this time, the solvent was removed under vacuum, and the resulting residue was washed with $CHCl_3$ to remove excess $[NEt_4]Br^+$. The residue was dissolved in water, and the crude product was purified by preparative RP-HPLC on a Waters μ Bondapak C_{18} (19 mm × 150 mm) column at a flow rate of 5 mL min^{-1} using a gradient of aqueous 0.1% CF_3COOH/MeOH as the eluent. Gradient: t = 0–5 min: 10% MeOH; 5–30 min: 10 → 100% MeOH; 30–34 min: 100% MeOH; 34–35 min: 100 → 10% MeOH; 35–40 min: 10% MeOH. Evaporation of the solvent in vacuum gave **I** as a colorless clear oil. Yield: 50 mg, 71%. ^{1}H NMR (D_2O, δ): 6.01 [s, 1H, H(4)pz], 5.07 (q br, 1H, NH), 4.33 (dd, 1H, CH^a), 4.07 (m, 1H, $CH^{a'}$), 3.62 (s br, 1H, NH), 3.50 (m, 1H, CH^g), 3.37 (m, 2H, $CH^{g'}$ + CH^b), 3.05 (s br, 1H, CH^d), 2.72 (d, 2H, CH^c + $CH^{c'}$), 2.54 (t br, 1H, $CH^{b'}$), 2.37 (m br, 1H, $CH^{d'}$), 2.33 (t, 2H, CH^e + $CH^{e'}$), 2.24 (s, 3H, CH_3pz), 2.14 (s, 3H, CH_3pz), 2.04 (m, 1H, CH^f), 1.88 (m, 1H,

$CH^{f'}$). ^{13}C NMR (D_2O, δ): 196.6, 196.2, 196.1 (C≡O), 179.8 (CO), 155.7 [C(3/5)pz], 146.3 [C(3/5)pz], 109.8 [C(4)pz], 67.8 (C^g), 63.2 (C^c), 54.5 (C^b), 49.1 (C^a), 44.2 (C^d), 33.1 (C^e), 21.5 (C^f), 17.3 (CH_3pz), 12.9 (CH_3pz). The spectra were assigned with the help of 2D experiments (^1H–^1H correlation spectroscopy, COSY, and ^1H–^{13}C heteronuclear single quantum coherence, HSQC). IR (KBr, ν/cm^{-1}): 2031, 1974, 1901 (C≡O), 1686, 1432, 1205, 1143, 848, 800, 728, 588. ESI-MS (+) (referenced to the species with ^{187}Re; relative abundance in parentheses): m/z 539 (100%) $[M+H]^+$. Retention time: 18.6 min.

2. *Synthesis of the intermediate [Re(CO)$_3$(κ^3-pz-BPO-Et)]$^+$ (**II**).* To a solution of **I** (0.020 g, 0.037 mmol) and HOBt (8 mg, 0.056 mmol) in dry acetonitrile (5 mL) at 0–5 °C was added DCC (12 mg, 0.056 mmol), and the mixture was stirred for 30 min. After addition of 1-aminomethylenediphosphonic acid tetraethyl ester (17 mg, 0.056 mmol) dissolved in acetonitrile (approximately 1 mL), stirring was continued at room temperature. The RP-HPLC chromatogram revealed that the reaction was complete after 20 h. The DCC–urea precipitate was removed by centrifugation and the resulting solution evaporated. The crude residue was dissolved in a H_2O/CH_3CN (90:10) mixture, filtered to discard the remaining DCC–urea and purified by preparative RP-HPLC on a Waters μ Bondapak C_{18} (19 mm × 150 mm) column at a flow rate of 5 mL min^{-1}. UV detection, 254 nm; eluent A 0.5% CF_3COOH solution, eluent B 0.5% CF_3COOH solution in acetonitrile; method, t = 0–3 min, 0% eluent B; 3–3.1 min, 0–25% eluent B; 3.1–9 min, 25% eluent B; 9–9.1 min, 25–34% eluent B; 9.1–20 min, 34–100% eluent B; 20–24 min, 100% eluent B; 24–26 min, 100–0% eluent B; 26–30 min, 0% eluent B. Evaporation of the solvent in vacuum gave intermediate **II** as a colorless clear oil. Yield: 20 mg, 66%. ^1H NMR (D_2O, δ): 6.01 [s, 1H, H(4)pz], 5.04 (s br, 1H, NH), 4.51 (m, 1H, CH^h), 4.28 (d br, 1H, CH^a), 4.08 (m, 8H, P–OC$\underline{H}_2$CH$_3$), 3.94 (m, 1H, $CH^{a'}$), 3.64 (m br, 1H, NH), 3.54 (m br, 1H, CH^g), 3.29 (m br, 2H, $CH^{g'}$ + CH^b), 3.00 (m br, 1H, CH^d), 2.71 (s br, 2H, CH^c + $CH^{c'}$), 2.54 (t br, 1H, $CH^{b'}$), 2.35 (m br, 1H, $CH^{d'}$), 2.33 (t, 2H, CH^e + $CH^{e'}$), 2.25 (s, 3H, CH_3pz), 2.13 (s, 3H, CH_3pz), 2.04 (m br, 1H, CH^f), 1.83 (m br, 1H, $CH^{f'}$), 1.15 (m, 12H, P–OCH$_2$C$\underline{H}_3$). ^{13}C NMR (D_2O, δ): 3× ~196.1 (C≡O), 179.5 (CO), 155.6 [C(3/5)pz], 146.2 [C(3/5)pz], 109.7 [C(4)Pz], 67.7 (C^g), 67.5 (P–O$\underline{C}$H$_2$CH$_3$), 63.1 (C^c), 54.5 (C^b), 50.1 (C^h, P–CH–P), 49.0 (C^a), 44.1 (C^d), 32.7 (C^e), 21.3 (C^f), 17.7 (P–OCH$_2$C$\underline{H}_3$), 17.3 (CH_3pz), 12.8 (CH_3pz). The spectra were assigned with the help of 2D experiments (^1H–^1H COSY and ^1H–^{13}C HSQC). ^{31}P NMR (D_2O, δ): 17.9 (s). Retention time: 16.1 min.

3. *Synthesis of **3**.* To a suspension of **II** (20 mg, 0.024 mmol) in dry dichloromethane (5 mL) at 0 °C was added dropwise trimethylsilyl bromide (0.5 mL, 3.7 mmol). The mixture was allowed to warm up to room temperature and stirred overnight. The solvent was evaporated, and the residue was treated with methanol (5 mL) for 1.5 h with stirring. The methanol was removed by evaporation and the crude product was washed with chloroform. Complex **3** was obtained as a pale yellow oil. Yield: quantitative, based on the ^1H NMR spectrum. ^1H-NMR (D_2O, δ): 6.01 [s, 1H, H(4)pz], 5.04 (s br, 1H, NH), 4.53 (m, 1H, CH^h), 4.29 (d br, 1H, CH^a), 4.07 (m br, 1H, $CH^{a'}$), 3.64 (s br, 1H, NH), 3.50 (m br, 1H, CH^g), 3.26 (m br, 2H, $CH^{g'}$ + CH^b), 3.01 (m br, 1H, CH^d), 2.71 (s br, 2H, CH^c + $CH^{c'}$), 2.55 (t br, 1H, $CH^{b'}$), 2.34 (m br, 1H, $CH^{d'}$), 2.24 (s, 3H, CH_3pz), 2.20 (s br, 2H, CH^e + $CH^{e'}$), 2.13 (s, 3H, CH_3pz), 2.03 (m, 1H, CH^f), 1.88 (m br, 1H, $CH^{f'}$). ^{13}C NMR (D_2O, δ): 196.5, 196.1, 194.9 (C≡O), 180.4 (CO), 155.6 [C(3/5)pz], 146.2 [C(3/5)pz], 109.7 [C(4)Pz], 67.7 (C^g), 63.2 (C^c), 54.6 (C^b), 50.9 (C^h, P-CH-P), 49.0 (C^a), 44.2 (C^d), 33.9 (C^e), 22.1 (C^f), 17.3 (CH_3pz), 12.9 (CH_3pz). The spectra were assigned with the help of 2D experiments (^1H–^1H COSY and ^1H–^{13}C HSQC). ^{31}P NMR (D_2O, δ): 11.1 (broad signal). Retention time: 13.9 min.

X-ray crystallographic analysis

A colorless crystal of **1**, suitable for X-ray diffraction analysis, was obtained from a mixture of $CHCl_3$/*n*-hexane and fixed inside a thin-walled glass capillary. Crystallography cell constants were determined by a least-squares fit to the setting parameters of 25 independent reflections, measured at room temperature using an Enraf–Nonius CAD4 diffractometer using graphite monochromated Mo Kα radiation (0.71073 Å) and operating in the $\omega - 2\theta$ mode. Empirical absorption correction (ψ scans) and data reduction were performed with the WINGX [30] suite of programs. The structures were solved by direct methods with SIR97 [31] and refined by full-matrix least-squares analysis with SHELXL97 [32]. Non-hydrogen atoms were refined with anisotropic thermal parameters, whereas hydrogen atoms were placed in idealized positions and allowed to be refined riding on the parent carbon atom. One remaining residual peak was assigned as an oxygen atom of one water molecule. The solvent oxygen was refined anisotropically and the corresponding hydrogen atoms were ignored. Molecular graphics were prepared using ORTEP3 [33]. A summary

of the crystal data, structure solution and refinement parameters is given in Table 1, and selected bond lengths and angles appear in Table 2.

Synthesis of the ^{99m}Tc-complexes (**1a**–**3a**)

A volume of 950 μl of the organometallic precursor *fac*-$[^{99m}Tc(OH_2)_3(CO)_3]^+$ in phosphate buffer pH 7.4 (**1a** and **2a**) or in saline pH 7.4 (**3a**), and 50 μL of a 10^{-3} M solution of pz-MPOEt, in ethanol, or aqueous solutions of pz-MPOH or pz-BPOH were placed in a 10-mL glass vial under nitrogen. The vial was then heated to 100 °C for 30 min, cooled on an ice bath and the final solution was analyzed by RP-HPLC. Retention times: 16.3 min (**1a**), 11.4 min (**2a**) and 13.2 min (**3a**).

Plasma stability in vitro

3a (100 μL) was added to 500 μL of human plasma and incubated at 37 °C. After incubation (0, 1, 2 and 4 h), aliquots (100 μL) were taken and the plasma proteins precipitated with ethanol (200 μL). The plasma was centrifuged at 3,000 rpm for 15 min at 4 °C and the supernatant (protein-free plasma) filtered trough a Millipore filter (0.22 μm), and was analyzed by RP-HPLC.

Biodistribution studies

The in vivo behavior of complexes **1a**–**3a** was evaluated in groups of four to five female CD-1 mice (randomly bred, Charles River) weighing approximately 20–25 g each. The animals were injected intravenously with 100 μL (7.0–18.5 MBq) of each preparation via the tail vein and were maintained on normal diet ad libitum. All animal studies were conducted in accordance with the highest standards of care, as outlined in European law. Mice were killed by cervical dislocation at 1 and 4 h after injection. The injected radioactive dose and the radioactivity remaining in the animal it being killed were measured with a dose calibrator (Aloka, Curiemeter IGC-3, Tokyo, Japan). The difference between the radioactivity in the injected and the killed animal was assumed to be due to total excretion from whole animal body. Blood samples were taken by cardiac puncture when the animals were killed. Tissue samples of the main organs were then removed, weighed and counted using a γ counter (Berthold). Biodistribution results were expressed as the percentage of the injected dose (ID) per gram of tissue. For blood, bone and muscle, total activity was calculated assuming that these organs constitute 6, 10 and 40% of the total weight, respectively. The remaining activity in the carcass was also measured with a dose calibrator. Blood samples, collected when the animals were killed, were centrifuged, the serum separated and treated with ethanol to precipitate the proteins and the supernatant was analyzed by HPLC, as described already for the in vitro plasma stability evaluation. The urine samples were filtered trough a Millipore filter (0.22 μm) and were also analyzed by RP-HPLC.

Table 1 Crystallographic data for complex **1**

Formula	$C_{18}H_{31}ClN_4O_7PRe$
M (g mol^{-1})	668.09
Crystal system	Monoclinic
Space group	$P21/n$
a (Å)	13.5880(17)
b (Å)	13.7897(10)
c (Å)	14.870(3)
α (°)	90
β (°)	106.929(9)
γ (°)	90
V (Å^3)	2665.4(7)
Z	4
T (°C)	21(2)
ρ (calculated) (g cm^{-3})	1.665
μ (Mo Kα) (mm^{-1})	4.760
Reflections collected	5,989
Independent reflections	5,745 (R_{int} = 0.0355)
Parameters	293
R^a	0.0551(0.1073)[b]
wR_2[a]	0.0867(0.1014)[b]

[a] The values were calculated for data with $I > 2\sigma(I)$

[b] Based on all data

Table 2 Selected bond lengths (angstroms) and angles (degrees) for the cation of complex **1**

Re(1)–C(3)	1.876(11)	Re(1)–C(2)	1.895(10)
Re(1)–C(1)	1.895(9)	Re(1)–N(4)	2.176(6)
Re(1)–N(1)	2.201(6)	Re(1)–N(3)	2.258(6)
C(1)–O(1)	1.159(9)	C(2)–O(2)	1.155(10)
C(3)–O(3)	1.159(11)		
C(3)–Re(1)–C(2)	87.3(4)	C(3)–Re(1)–C(1)	88.5(4)
C(2)–Re(1)–C(1)	86.6(4)	C(3)–Re(1)–N(4)	174.2(3)
C(2)–Re(1)–N(4)	98.4(4)	C(1)–Re(1)–N(4)	93.0(3)
C(3)–Re(1)–N(1)	92.4(3)	C(2)–Re(1)–N(1)	95.1(3)
C(1)–Re(1)–N(1)	178.1(3)	N(4)–Re(1)–N(1)	86.0(2)
C(3)–Re(1)–N(3)	95.8(3)	C(2)–Re(1)–N(3)	176.1(4)
C(1)–Re(1)–N(3)	91.2(3)	N(4)–Re(1)–N(3)	78.5(2)
N(1)–Re(1)–N(3)	87.1(2)		

Results and discussion

Synthesis and characterization of the phosphonate-containing conjugates pz-MPOH and pzBPOH

As mentioned already, the ^{99m}Tc-labeled phosphonates in clinical use consist of a mixture of species, most likely with polymeric structure, which have not yet been fully characterized. The metal is believed to be in a higher oxidation state, most presumably +IV [34] and, in vivo, the phosphonate groups are not exclusively used to bind to the bone but are also used to coordinate to the metal in such chemical species. In the case of the lower oxidation states, namely, in the case of the *fac*-[^{99m}Tc(CO$_3$)]$^+$ core, P–O–Tc coordination has also been observed [35]. In order to label BPs with the *fac*-[^{99m}Tc(CO$_3$)]$^+$ core and to discharge the possibility of unspecific coordination of the phosphonic acid groups to the metal, we have taken advantage of both the coordination properties of the pyrazolyl-containing chelators and of the remarkable stability (in vitro and in vivo) shown by the ^{99m}Tc tricarbonyl complexes anchored by such ligands [21, 23, 24]. Thus, on the basis of the concept of a bifunctional chelating approach, we designed and synthesized the pz-MPOEt and pz-MPOH model ligands, which contain, simultaneously, a MP moiety and the N,N,N donor-atom set of the pyrazolyl-containing backbone (Scheme 1). These compounds were prepared from the same common precursor, the pz(Boc)-MPOEt intermediate, which was obtained by direct alkylation of the secondary amine in 3,5-Me$_2$–pz(CH$_2$)$_2$NH(CH$_2$)$_2$ NH–Boc with diethyl (2-bromoethyl)phosphonate (Scheme 1). Selective deprotection of the Boc group in pz(Boc)-MPOEt with CF$_3$COOH afforded, in high yield (approximately 90%), the pz-MPOEt molecule as a pale yellow viscous oil, which is soluble in most organic solvents and almost completely insoluble in water. Treatment of the intermediate pz(Boc)-MPOEt with trimethylsilyl bromide, followed by hydrolysis with MeOH/H$_2$O yielded pz-MPOH as a highly water soluble white solid. Both MP-containing ligands were thoroughly characterized by the usual analytical techniques in chemistry, as described in ''Materials and methods.''

Synthesis and characterization of the Re tricarbonyl complexes with the pz-MPOEt and pz-MPOH conjugates

Considering that the presence of a MP moiety could modify the coordination mode of the N,N,N donor-atom set of the pyrazolyl-containing backbone towards the core *fac*-[M(CO$_3$)]$^+$ (M is ^{99m}Tc, Re), we decided to study reactions of the organometallic precursor [ReBr(CO)$_5$] with pz-MPOEt and pz-MPOH. We found that these two compounds react with the precursor affording the cationic complexes [Re(CO)$_3$(κ^3-pz-MPOEt)]$^+$ (**1**) and [Re(CO)$_3$(κ^3-pz-MPOH)]$^+$ (**2**) (Scheme 2).

Complex **1**, obtained as an air-stable hygroscopic white solid, was characterized by the usual analytical techniques, including X-ray diffraction analysis. The pz-MPOEt ligand coordinates as neutral and tridentate through the nitrogen atoms of the pyrazolyl–diamine ligand backbone. The facial arrangement of the carbonyl groups in **1** is evidenced by the CO-stretching absorptions in the IR spectra [18, 22]. The ν(CO) stretching bands appear at 2,098, 2,027 and 1,901 cm^{-1}. These values are within the range normally found for other complexes with the moiety ''*fac*-Re(CO)$_3$.'' As expected, the ^{31}P NMR spectrum in CD$_3$OD shows only one singlet at δ 29.4, which is slightly shifted to higher field relative to the chemical shift of the free ligand pz-MPOEt (δ 32.8). The most important feature of the ^{1}H NMR spectrum of complex **1** is related to the diastereotopic character of the protons of the primary amine (δ 5.57, 1H; δ 3.80–3.68, 1H), and of most of the methylenic protons of the ligand backbone upon coordination to the metallic center (δ 4.54, 1H; δ 3.95–3.88, 1H; δ 3.43, 1H; δ 3.23–3.19, 1H; δ 2.96, 1H and δ 2.31–2.28, 1H). This behavior is typical for asymmetric pyrazolyl–diamine ligands with the N,X,N donor-atom set (X is S, N), and had already been observed in other tricarbonyl complexes, being strong evidence of ligand coordination [21–23].

The structure of the cationic complex [Re(CO)$_3$(κ^3-pz-MPOEt)]$^+$ (**1**) consists of ion-pair units in which the Re atom in the cation is in a distorted octahedral environment. An ORTEP view of the cation of complex **1** is shown in Fig. 1. Selected bond distances and angles are listed in Table 2.

The carbonyl groups occupy one triangular face of the coordination polyhedra, with the other three remaining coordination sites being defined by the tridentate pz-MPOEt ligand. In compound **1**, the chloride ion, which appears as a consequence of the replacement of the bromine atom during recrystallization from chloroform/*n*-hexane, forms hydrogen bonds with the primary amine. The N4...Cl distance and N–H–Cl angles are 3.153(6) Å and 158.1(4)°. Deviations from the ideal octahedral geometry can be seen on the bond angles around the Re atom (Table 1). The *cis* and *trans* bond angles range between 86.0(2) and 98.4(4)° and between 174.2(3) and 178.1(3)°, respectively. The Re–C distances are almost identical, spanning from 1.876(11) to 1.895(9) Å, being comparable with the values found for other Re(I) tricarbonyl complexes anchored by pyrazolyl-based ligands that we have previously reported [21–23]. The Re–N4 bond distance in **1** [2.176(6) Å] is, as expected, slightly shorter than the distance between the metal and the nitrogen atom of the secondary amine in **1** [Re–N(3), 2.258(6) Å]. The Re–N1 bond distance in **1** is comparable with the values

Scheme 1 Synthesis of the monophosphonate-containing conjugates pz-MPOEt and pz-MPOH

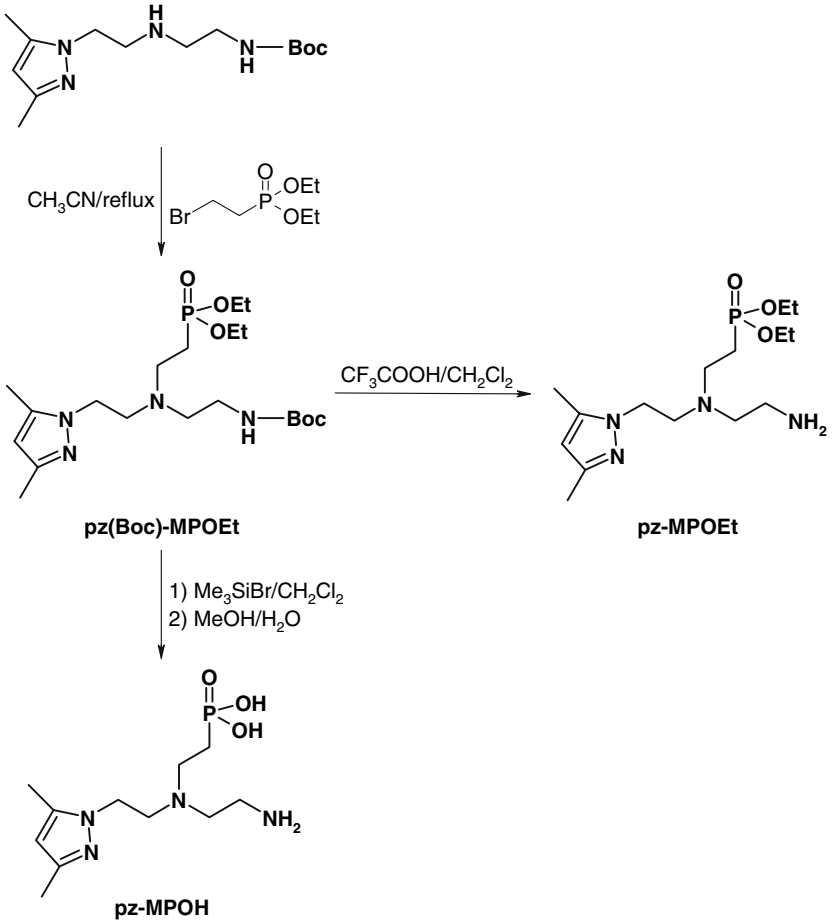

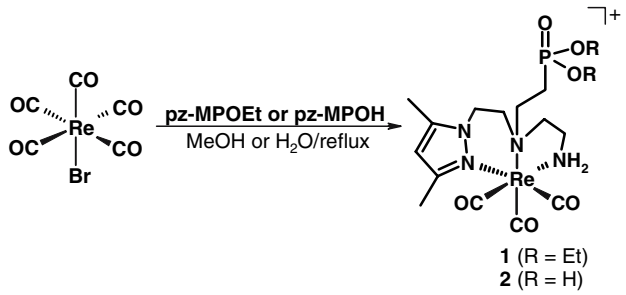

Scheme 2 Preparation of the rhenium tricarbonyl complexes **1** and **2**

reported for Re–Npz* of other Re(I) complexes containing pyrazolyl-based ligands [21–23].

Owing to unfavorable kinetics, even after several attempts, we were not able to isolate the organometallic complex $[Re(CO)_3(\kappa^3\text{-pz-MPOH})]^+$ (**2**) in a pure form. In fact, after refluxing stoichiometric amounts of pz-MPOH with $[Re(CO)_5Br]$ in water, for 18 h, two chemical species could be identified by RP-HPLC and $^1H/^{31}P$ NMR spectroscopy. One of the species was the free ligand (pz-MPOH), as indicated by its RP-HPLC chromatogram and multinuclear NMR spectra, which were in excellent agreement with those of an authentic sample. The other species formed was formulated as $[Re(CO)_3(\kappa^3\text{-pz-MPOH})]^+$ (**2**), mainly on the basis of the $^1H/^{31}P$ NMR spectra (see ''Materials and methods''). In the ^1H NMR spectrum of **2**, the presence of the azolyl ring resonances and the characteristic diastereotopic splitting pattern for the methylenic and amine protons of the coordinated pz-MPOH could be easily assigned. Such a pattern, comparable with that of complex **1**, is consistent with a tridentate coordination mode for the ligand. The ^{31}P NMR spectrum of complex **2** in D_2O shows only one singlet at δ 23.4 ppm, which is shifted downfield (Δ = 3.1 ppm) relative to the shift of the free pz-MPOH. This shift is of the same order of magnitude as that observed for the structurally characterized complex **1** (Δ = 3.4 ppm) in CD_3OD. These results also confirm that the phosphonic acid group is not involved in the coordination to the metal. In fact, the Δ values found for **1** and **2** are far below the range previously found for organometallic Re(I) complexes directly stabilized by phosphonic acids (Δ = 16–30 ppm) [35]. These data allowed us to conclude that, under the conditions studied, the pz-MPOH ligand coordinates to the metal center most likely through the N,N,N donor-atom set, and no unspecific

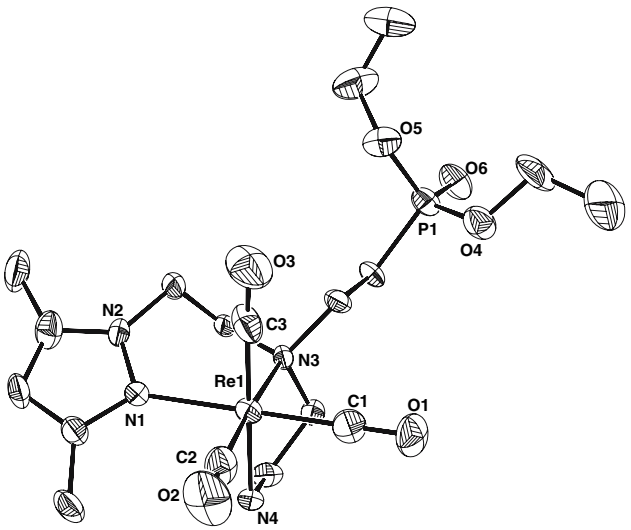

Fig. 1 ORTEP view of complex **1** with selected atoms numbered; *thermal ellipsoids* are drawn at the 30% probability level

interactions occur between the phosphonic acid group and the metallic center. Thus, on the basis of these results, we designed the bifunctional chelating agent pz-BPOH. The conjugate was prepared according to the general procedure outlined in Scheme 3.

The first step involves the preparation of the pz(Boc)-BPOEt intermediate by conjugation of aminomethylenediphosphonic acid tetraethyl ester with the bifunctional pyrazolyl-containing chelator 3,5-Me_2pz$(CH_2)_2$–N$((CH_2)_3$ COOH$)(CH_2)_2$–NH–Boc using HOBt and DCC as coupling reagents. Simultaneous removal of the Boc and ethyl ester protective groups was achieved in one-pot reaction using trimethylsilyl bromide under appropriate experimental conditions. The final BP-containing ligand pz-BPOH was obtained in the form of a white solid soluble in water and alcohols, and insoluble in most organic solvents. The structures of both the intermediate ligand pz(Boc)-BPOEt and the final product pz-BPOH were confirmed after thorough characterization by IR and $^{1}H/^{13}C/^{31}P$ NMR spectroscopy, and elemental analysis. The characteristic splitting pattern of the peak at δ 5.19 (triplet of doublets), assigned to the C<u>H</u> proton of the phosphonate unit in pz(Boc)-BPOEt, and the corresponding coupling constants ($^{2}J_{PH}$ = 22.2, $^{3}J_{HH}$ = 10.2) observed in the ^{1}H NMR spectrum are obvious evidence for amide bond formation during the coupling reaction. In the case of the pz-BPOH conjugate, the ^{1}H NMR spectrum in D_2O presents the typical sharp singlet peaks for the H(4) proton (δ 6.07) and the methyl groups of the pyrazolyl ring (δ 2.20 and δ 2.14). Broad resonances for the methylenic protons of the backbone are also observed. The ^{13}C spectrum shows 14 peaks, which correspond to all the carbon nuclei of the ligand. A single peak (δ 13.7) for the two phosphorus nuclei present in the molecule can be found in the ^{31}P NMR spectrum. The IR spectrum of pz-BPOH presents two strong bands at about 1,647 and 1,154 cm^{-1} assigned to the ν(C=O) and ν(P=O) stretching bands of the amide and phosphonic acid groups, respectively.

In order to establish unambiguously the coordination mode of the ligand pz-BPOH towards the metallic core *fac*-$[M(CO)_3]^+$ (M is Re, ^{99m}Tc), and to concomitantly prove that the BP pendant moiety is not complexing the metal, we developed two different synthetic approaches to isolate the rhenium organometallic complex **3** in a pure form (Scheme 4). In the so-called direct method, we reacted a stoichiometric amount of pz-BPOH with the recently described organometallic precursor $[Re(CO)_3(H_2O)_3]Br$ in refluxing water overnight [29]. After full evaporation of the solvent, the crude product obtained was dissolved in a H_2O/acetonitrile mixture (90:10) and purified by semipreparative RP-HPLC, giving complex **3** in approximately 50% yield. The same complex has also been obtained in high yield via an indirect method, using the well-characterized organometallic complex **I** as starting material [23]. The coupling of the BP moiety to the pendant carboxylic acid group was accomplished by reacting **I** with 1-aminomethylenediphosphonic acid tetraethyl ester in the presence of the activating agent HOBt to give the intermediate complex **II**. Complex **3** was then obtained by direct hydrolysis of the tetraethyl esters in **II** with trimethylsilyl bromide. It is worth noting the high stability exhibited by the rhenium tricarbonyl complexes **II** and **3** in the presence of trimethylsilyl bromide, a strong Lewis acid.

Complex **3** was obtained in both cases as an air-stable, pale yellow clear oil, and was thoroughly characterized by $^{1}H/^{13}C/^{31}P$ NMR spectroscopy. The purity (above 92%) of the isolated compound in both synthetic methods was ascertained by analytical RP-HPLC (retention time 13.9 min). The use of 2D NMR experiments (^{1}H–^{1}H COSY and ^{1}H–^{13}C HSQC) was crucial for the assignments of the NMR spectra, and for full characterization of the compound. The ^{31}P NMR spectrum shows only one very broad singlet at approximately δ 11.1 (D_2O), which is slightly shifted to higher field relative to the chemical shift of the free ligand pz-BPOH (δ 13.7). The ^{1}H NMR spectrum of the product in D_2O presents the typical singlet peak at δ 6.01 assigned to the H(4) of the azole ring and the two characteristic singlet peaks at δ 2.24 and δ 2.13 assigned to the methyl groups of the pyrazolyl ring. The diastereotopic splitting pattern of the amine and of the methylenic protons could also be observed, and all signals were properly attributed (see ''Materials and methods''). The NMR data obtained for complex **3** are consistent with the tridentate coordination mode of the pyrazole–diamine ligand backbone, and no unspecific interactions between the pendant bisphosphonic acid group and the metal could be detected.

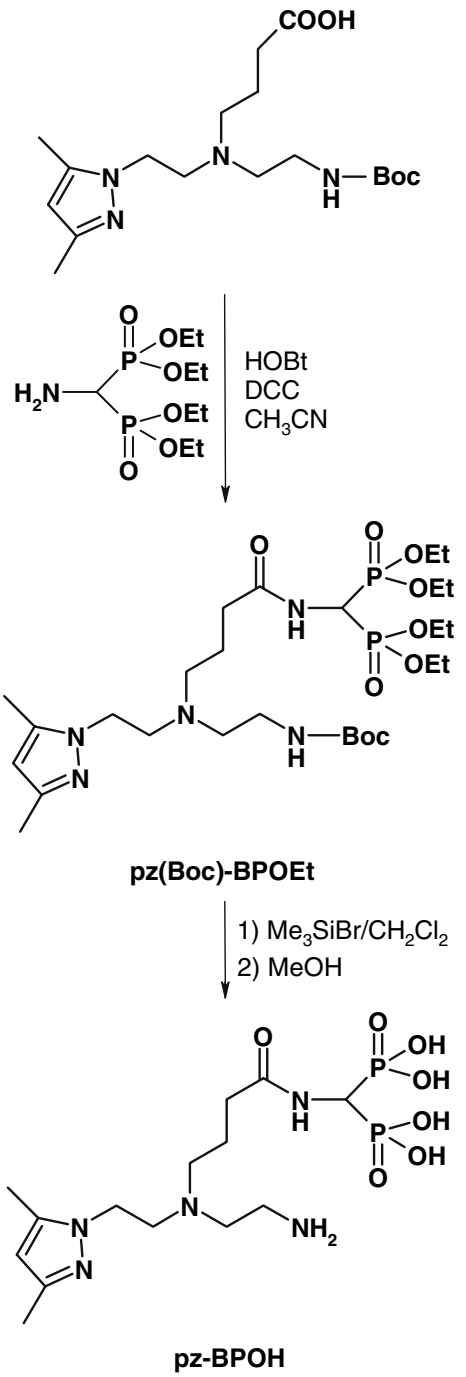

Scheme 3 Synthesis of the bisphosphonate-containing conjugate pz-BPOH

Synthesis and characterization of the ^{99m}Tc building blocks

In phosphate-buffered aqueous solutions (pH 7.4), or in saline pH 7.4 or pz-MPOEt, pz-MPOH and pz-BPOH react at 100 °C with the precursor *fac*-$[^{99m}Tc(CO)_3(OH_2)_3]^+$ giving in high yields **1a**, **2a** and **3a** as single well-defined species (Table 3).

The chemical identity of the complexes **1a**–**3a** was confirmed by comparison of their HPLC profiles with those of the corresponding rhenium complexes (**1**–**3**), previously synthesized and characterized (Table 3).

Evaluation in vitro and in vivo of the ^{99m}Tc complexes **1a**–**3a**

The stability of the organometallic radioactive model complexes **1a** and **2a**, obtained in high radiochemical yield, was evaluated in vitro. As expected for complexes anchored on pyrazolyl–diamine chelators, the model complexes **1a** and **2a** show great stability in vitro under physiologic conditions. No decomposition products or reoxidation to pertechnetate was observed by RP-HPLC analysis, even after incubation of the radioactive complexes in phosphate-buffered saline (pH 7.4, 37 °C, 24 h) or in human plasma (37 °C, 4 h). These data, together with the high in vivo stability shown by other bioorganometallic complexes stabilized by pyrazolyl-containing ligands [15–18], prompted us to pursue the in vivo biological studies, and to evaluate tissue distribution of complexes **1a**–**3a** in view of the bone affinity and the uptake and clearance from major organs. Biodistribution studies of **1a**–**3a** were performed in groups of four to five mice, in order to assess the effect of the MP/BP pendant arm on their ability to bind to bone. For comparative purposes, the biodistribution of the bone-imaging radiopharmaceutical ^{99m}Tc-MDP was also studied in the same animal model. The organ distribution (percentage of the ID per gram) of **1a**–**3a** and of ^{99m}Tc-MDP as a function of time is summarized in Table 4.

Rapid blood clearance and rapid washout from main organs, except those related to excretion, were found for the complexes **1a**–**3a**. Additionally, none of them presented a high level of stomach radioactivity indicating good in vivo stability. The main differences are related to the main excretory route and the whole-body total excretion. Complexes **1a** and **2a** have a significantly higher hepatobiliar uptake than complex **3a**. The liver radioactivity rapidly clears into the intestines, suggesting the hepatobiliar tract is the main excretory pathway for those complexes, while complex **3a** seems to be eliminated via the urinary pathway. Furthermore, complex **3a** showed the fastest total excretion (72.0 ± 1.8 and 74.1 ± 1.3% at 1 and 4 h after injection, respectively). Complex **3a** showed a rapid accumulation and long residence in the bone, and its uptake by this organ was significantly higher than those of **1a** and **2a**, certainly owing to the presence of the BP pendant arm in the molecular structure of the ligand. This high accumulation of radioactivity in bone, as well as the high bone-to-blood (18) and bone-to-muscle (38) ratios, suggests the potential of **3a** as a bone-seeking agent.

Scheme 4 Synthesis of the rhenium tricarbonyl complex **3**. The identification system for NMR assignments is displayed

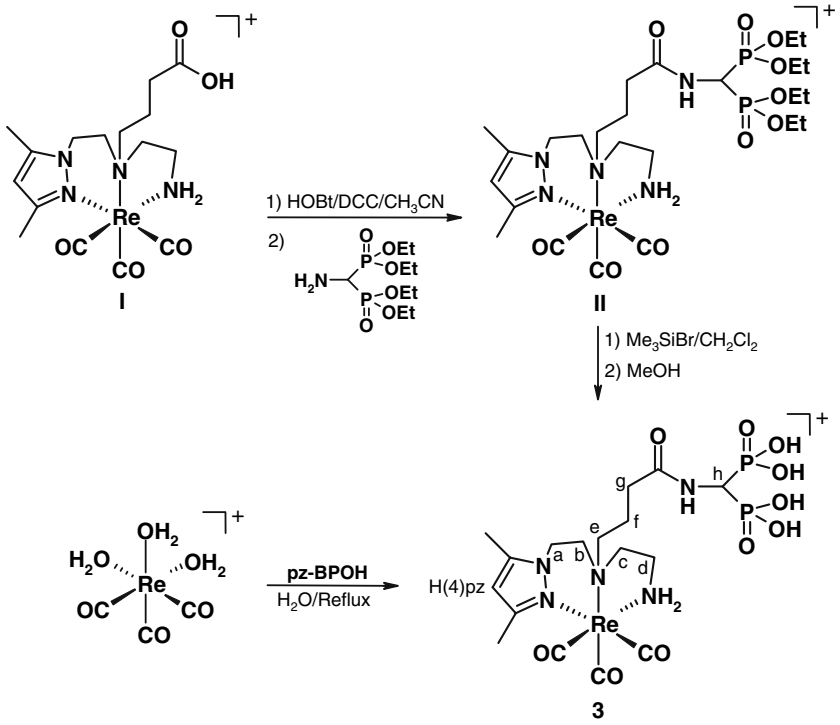

However, the comparative analysis of the biodistribution data and those obtained with ^{99m}Tc-MDP, in the same animal model, indicated a similar biokinetics profile, but a significantly lower bone uptake.

To verify the in vivo stability of complexes **1a**–**3a**, samples of murine serum and urine collected when the mice were killed were also analyzed by radiometric RP-HPLC. The murine serum, isolated from blood collected 60 min after intravenous administration, did not show any traces of pertechnetate, and more than 95% of the radioactivity could be assigned to the complexes. Analysis of urine collected when the mice were killed (60 min) demonstrated again high in vivo stability of the complexes, because no metabolites could be detected. As an example, the HPLC chromatograms of urine samples collected from mice injected with **2a** and **3a** are shown in Fig. 2. The resistance to metabolic degradation in blood and the excretion of the ^{99m}Tc tricarbonyl complexes intact into the urine demonstrate their high in vivo robustness.

Table 3 Experimental conditions for the synthesis of complexes **1a**–**3a** and retention times of the complexes in the reversed-phase high-performance liquid chromatography (*RP-HPLC*) chromatograms

Complex	Labeling conditions			Yield (%)	RP-HPLC retention times (min)
	Time (min)	Temperature (°C)	[L] (M)		
1a	30	100	5×10^{-5}	>96	16.3 (15.8)[a]
2a				>98	11.4 (10.8)[a]
3a				>96	13.2 (13.9)[a]

[a] Re complexes

Conclusions

We have developed a promising organometallic radiocomplex (**3a**), which comprises a pyrazolyl-containing backbone with a N,N,N donor-atom set for metal stabilization and a pendant bisphosphonic acid group for bone binding (pz-BPOH). The complex is a single, well-defined chemical species, which was been identified by comparison of its chromatographic behavior with that of the rhenium analogue **3**. Complex **3a** is stable in vivo, without any measurable decomposition or reoxidation. Biodistribution studies of the radiocomplex in mice indicated a fast rate of blood clearance and high rate of total radioactivity excretion, occurring primarily through the renal–urinary pathway. Despite the moderate bone uptake (3.04 ± 0.47% ID g^{-1} organ, 4 h after injection), the high stability presented by the radioactive probe **3a** and its adequate in vivo pharmacokinetics, namely, its favorable bone-to-blood and bone-to-muscle ratios, encourages the search for new ligands with the same chelating unit (pyrazolyl-containing backbone), but bearing other bisphosphonic acid pendant arms, with higher bone affinity, namely, 1-hydroxy-1,1-bisphosphonates.

Table 4 Biodistribution data of complexes **1a–3a** and ^{99m}Tc-MDP in mice at 60 and 240 min after injection (percentage of the injected dose per gram ± standard deviation)

	1a		**2a**		**3a**		^{99m}Tc-MDP	
	60 min	240 min	60 min	240 min	60 min	240 min	60 min	240 min
Blood	0.80 ± 0.18	0.60 ± 0.07	0.51 ± 0.20	0.20 ± 0.04	0.47 ± 0.08	0.17 ± 0.01	0.35 ± 0.07	0.14 ± 0.04
Liver	5.59 ± 1.44	4.47 ± 0.26	10.11 ± 1.39	3.48 ± 1.42	0.89 ± 0.12	0.82 ± 0.28	0.23 ± 0.12	0.22 ± 0.07
Intestine	20.43 ± 2.93	18.50 ± 4.54	10.14 ± 1.68	13.80 ± 6.19	0.42 ± 0.10	0.59 ± 0.17	0.45 ± 0.24	0.37 ± 0.07
Spleen	2.05 ± 0.61	2.23 ± 0.14	0.11 ± 0.02	0.42 ± 0.18	0.52 ± 0.20	0.19 ± 0.07	0.15 ± 0.05	0.08 ± 0.02
Heart	0.32 ± 0.05	0.28 ± 0.03	0.22 ± 0.05	0.17 ± 0.02	0.19 ± 0.02	0.10 ± 0.02	0.50 ± 0.40	0.10 ± 0.02
Lung	0.87 ± 0.29	0.75 ± 0.11	0.41 ± 0.12	0.23 ± 0.05	0.48 ± 0.06	0.31 ± 0.19	1.90 ± 0.40	0.15 ± 0.03
Kidney	4.11 ± 1.81	1.26 ± 0.44	2.83 ± 0.31	1.23 ± 0.29	1.86 ± 0.49	1.54 ± 0.57	1.30 ± 0.30	0.86 ± 0.38
Muscle	0.12 ± 0.02	0.10 ± 0.07	0.04 ± 0.02	0.02 ± 0.01	0.13 ± 0.04	0.08 ± 0.06	0.70 ± 0.20	0.32 ± 0.12
Bone	0.18 ± 0.04	0.16 ± 0.07	0.21 ± 0.04	0.12 ± 0.01	2.74 ± 0.71	3.04 ± 0.47	6.40 ± 2.00	8.41 ± 1.07
Stomach	0.68 ± 0.31	0.37 ± 0.06	0.78 ± 0.30	0.42 ± 0.05	0.46 ± 0.26	0.50 ± 0.28	1.40 ± 0.10	0.37 ± 0.03

MDP methylenediphosphonate

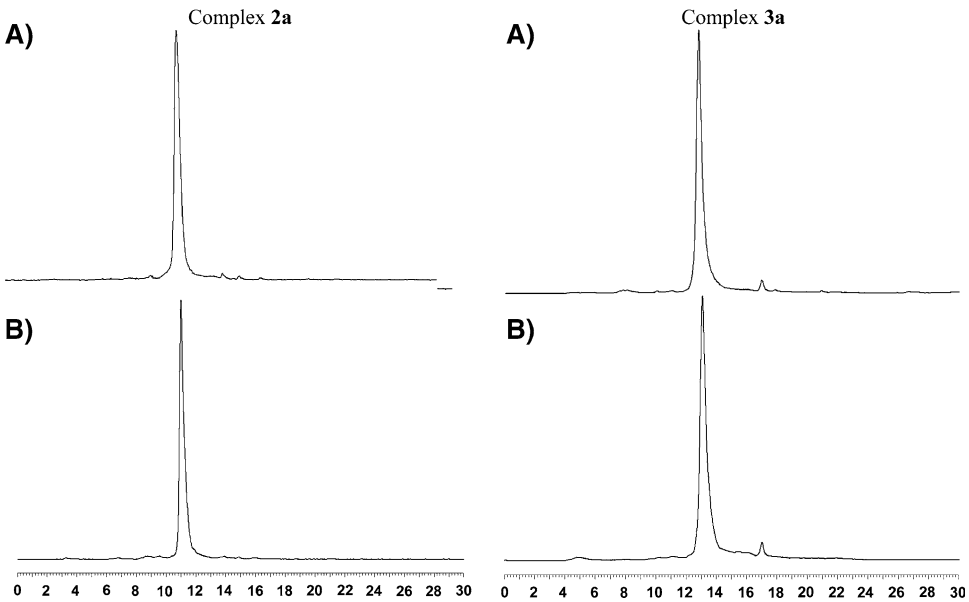

Fig. 2 Reversed-phase high-performance liquid chromatography radioactive traces (γ detection) for complexes **2a** and **3a**: *A* injected preparation and *B* urine sample collected 60 min after injection

Supplementary material

Crystallgraphic data (without structure factors) for the structure reported in this paper have been deposited with the Cambridge Crystallographic Data Centre as supplementary publication no. CCDC-622301. Copies of the data can be obtained free of charge from the CDCC (12 Union Road, Cambridge CB2 1EZ, UK; tel.: (+44) 1223-336-408; fax: (+44) 1223-336-003; e-mail: deposit@ccdc.cam.ac.uk; website see link below http://www.ccdc.cam.ac.uk).

Acknowledgements This work was partially supported by the Fundação para a Ciência e Tecnologia (FCT) through the project POCI/SAU-FCF/58855/2004, and by COST ACTION B12. We thank Mallinkrodt-Tyco for financial support. B.L.O. and E.P. would like to thank the FCT for BI grants. We wish to acknowledge the Mass Spectrometry Laboratory for performing the electrospray ionization mass spectrometry determination at the Instituto de Tecnologia Química e Biológica, Universidade Nova de Lisboa, Oeiras, Portugal.

References

1. Love C, Din AS, Tomas MB, Kalapparambath TP, Palestro CJ (2003) Radiographics 23:341–358
2. Coleman RE (2001) Cancer Treat Rev 27:165–176
3. Pinski J, Dorff TB (2005) Eur J Cancer 41:932–940
4. Serafini AN (2001) J Nucl Med 42:895–906
5. Bagi CM (2005) Adv Drug Deliv Rev 57:995–1010
6. Reisfield GM, Silberstein EB, Wilson GR (2005) Am J Hos Palliat Med 22:41–46

7. Ogawa K, Mukai T, Asano D, Kawashima H, Kinuya S, Shiba K, Hashimoto K, Mori H, Saji H (2007) J Nucl Med 48:122–127
8. Uehara T, Jin ZL, Ogawa K, Akizawa H, Hashimoto K, Nakayama M, Arano Y (2007) Nucl Med Biol 34:79–87
9. Ogawa K, Mukai T, Arano Y, Otaka A, Ueda M, Uehara T, Magata Y, Hashimoto K, Saji H (2006) Nucl Med Biol 33:513–520
10. Ogawa K, Mukai T, Arano Y, Ono M, Hanaoka H, Ishino S, Hashimoto K, Nishimura H, Saji H (2005) Bioconjugate Chem 16:751–757
11. Ogawa K, Mukai T, Arano Y, Hanaoka H, Hashimoto K, Nishimura H, Saji H (2004) J Labelled Compd Radiopharm 47:753–761
12. Zhang S, Gangal G, Uluda H (2007) Chem Soc Rev (in press). doi:10.1039/b512310k
13. Verbeke K, Rozenski J, Cleynhens B, Vanbilloen H, Groot T, Weyns N, Bormans G, Verbruggen A (2002) Bioconjugate Chem 13:16–22
14. Shigematsu M, Shiomi S, Iwao H, Ochi H (2002) Ann Nucl Med 16:55–59
15. Doubsky J, Laznicek M, Laznickova A, Leseticky L (2004) J Radioanal Nucl Chem 260:53–59
16. El-Mabhouh A, Angelov CA, Cavell R, Mercer JR (2006) Nucl Med Biol 33:715–722
17. Santos I, Paulo A, Correia JDG (2005) Top Curr Chem 252:45–84
18. Alberto R (2005) Top Curr Chem 252:1–44
19. Schibli R, Schubiger AP (2002) Eur J Nucl Med 29:1529–1542
20. Garcia R, Gano L, Maria L, Paulo A, Santos I, Spies H (2006) J Biol Inorg Chem 11:769–782
21. Alves S, Paulo A, Correia JDG, Domingos Â, Santos I (2002) J Chem Soc Dalton Trans 4714–4719
22. Vitor RF, Alves S, Correia JDG, Paulo A, Santos I (2004) J Organomet Chem 689:4764–4774
23. Alves S, Paulo A, Correia JDG, Gano L, Smith CJ, Santos I (2005) Bioconjugate Chem 16:438–449
24. Alves S, Correia JDG, Santos I, Veerendra B, Sieckman GL, Hoffman, Rold T, Retzloff L, McCrate J, Prasanphanich A, Smith CJ (2006) Nucl Med Biol 33:625–634
25. Worms KH, Shmidt-Dunker M (1972) In: Kosolapoff GM, Maier L (eds) Organic phosphorus compounds, vol 7. Wiley, New York, chap 18
26. Kantoci D, Denike JK, Wechter WJ (1996) Synth Commun 26:2037–2043
27. Kubicek V, Rudovsky J, Kotek J, Hermann P, Vander LE, Muller RN, Kolar ZI, Wolterbeek HTh, Peters JA, Lukes I (2005) J Am Chem Soc 127:16477–16485
28. Alberto R, Schibli R, Egli A, Schubiger PA., Herrmann WA, Artus G, Abram U, Kaden TA (1995) J Organomet Chem 493:119–127
29. Lazarova N, James S, Babich J, Zubieta J (2004) Inorg Chem Commun 7:1023–1026
30. Farrugia LJ (1999) J Appl Crystallogr 32:837–838
31. Altomare A, Burla MC, Camalli M, Cascarano G, Giacovazzo G, Guagliardi A, Moliterini AGG, Polidoro G, Spagna R (1999) J Appl Crystallogr 32:115–119
32. Sheldrick GM,(1997) SHELXL-97. Program for the solution of crystal structure. University of Gottingen, Germany
33. Farrugia LJ (1997) J Appl Crystallogr 30:565
34. Alberto R (2004) In: McLeverty JA, Meyer TJ (eds) Comprehensive coordination chemistry II, vol 5. Elsevier–Pergamon, Amsterdam, pp 127–270
35. Mundwiler S, Waibel R, Spingler B, Kunze S, Alberto R (2005) Nucl Med Biol 32:473–484